

Fine-Tuned Conformation of Dithioacylpapain Intermediates: Insights from Resonance Raman Spectroscopy†

Munsok Kim, George I. Birnbaum, Rosemary C. Hynes,‡ Witold Neugebauer, and Paul R. Carey*

Contribution from the Institute for Biological Sciences, National Research Council of Canada, Ottawa, Ontario, Canada, K1A 0R6

Received December 4, 1992

Abstract: Interpretation of the resonance Raman (RR) spectrum of functioning *N*-benzoylglycine dithioacylpapain, ($C_6H_5C(=O)NHCH_2C(=S)SCH_2$ -papain) provides an estimate of four torsion angles near the point of catalytic attack. The torsion angles $CN-CC$, $NC-CS(\text{thiol})$, $CS-CC$, and $SC-C_{25}^{\alpha}N$ are -105° , $+15^\circ$, *gauche*⁻, and P_H (the hydrogen linked to C_{25}^{α} is in the *trans* position with respect to the thiol sulfur atom), respectively. Spectral interpretation relies on spectra–structure correlations derived from crystal structures of six *N*-acylglycine ethyl dithioesters, viz. *N*-acetylglycine, *N*-(β -phenylpropionyl)glycine, *N*-benzoylglycine (two forms), *N*-(*p*-methylbenzoyl)glycine, and *N*-(*p*-chlorobenzoyl)glycine ethyl dithioester, which have been examined by a combination of RR spectroscopic and X-ray crystallographic analyses. The structural conclusions are reached using three marker bands, near 1130, 680, and 550 cm^{-1} , in the RR spectrum of the dithioacylpapain and are supported by the intensity pattern of three additional marker bands in the 850–1050 cm^{-1} region. The value of $+15^\circ$ derived for the $NC-CS(\text{thiol})$ torsion angle in the acyl enzyme is outside the range of -22.2 to $+9.5^\circ$ observed in model *N*-acylglycine ethyl dithioesters and lies in the direction of the $NC-CS(\text{thiol})$ torsion angle for the transition state for deacylation. Thus, enzyme–substrate interactions cause a modest distortion of at least one torsion angle in the direction of the reaction pathway. In addition, crystal structure data for the six *N*-acylglycine ethyl dithioesters are discussed, including the newly determined structure of *N*-(*p*-methylbenzoyl)glycine ethyl dithioester. All dithioesters adopt so-called B-type conformations with small values for the $NC-CS(\text{thiol})$ torsion angle and short $N\cdots S(\text{thiol})$ nonbonded distances. The data reveal that correlated structural changes occur within the common $-C(=O)NHCH_2C(=S)SCH_2CH_3$ skeleton. These correlations involve bond lengths (e.g., $NC-CSS$), bond angles (e.g., $N-C-C$), and torsion angles (e.g., $NC-CS(\text{thiol})$) and are a consequence of the $N\cdots S(\text{thiol})$ nonbonded interaction. Importantly, they provide a basis for predicting the correlated changes in structural parameters in the dithioester moiety in the active site of the enzyme as it undergoes transformation along the reaction pathway.

Introduction

The resonance Raman spectra of dithioacylpapain intermediates provide access to structural information on the catalytically crucial region of the active site.^{1,2} By reacting substrates which are thionoesters, e.g., $RC(=O)NHCH_2C(=S)OCH_3$, with cysteine proteases such as papain, it is possible to generate dithioacyl enzymes, $RC(=O)NHCH_2C(=S)SCH_2$ -papain, in which the thiol sulfur is donated by papain's cysteine 25.³ The dithioester group in the active site has a λ_{max} near 315 nm, and excitation of the reaction mixture with 324-nm Kr^+ laser irradiation generates the resonance Raman (RR) spectrum of the dithioester moiety.¹ By these means we can observe selectively the vibrational spectrum of the group undergoing transformation in the active site. Analysis of the RR spectrum provides information on the torsion angles ϕ' , ψ , χ_2 , and χ_1 seen in Figure 1.^{2,4} Although the RR data can be gathered on a rapid time scale from the reaction mixture under turnover conditions, interpretation of the data is not always unambiguous. The principal means we have of overcoming this drawback is by combining X-ray crystallographic and Raman spectroscopic studies on model compounds that have spectral properties closely resembling those of the enzyme-

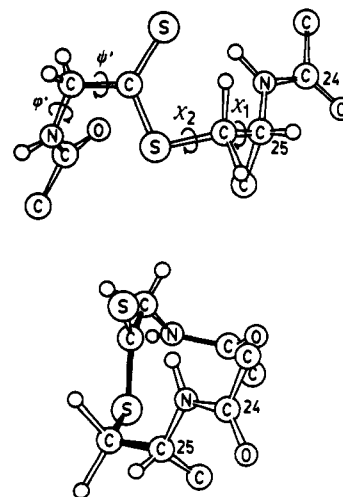


Figure 1. Two views of conformer B *gauche*- P_H with possible bond rotations about the ϕ' , ψ , χ_2 , and χ_1 torsional angles in the active site of the dithioacylpapain intermediates. The atoms attached to the alkyl side of the thiol sulfur are from active-site cysteine 25 and serine 24.

substrate intermediate.^{5,6} In this way we are able to set up exact structure–spectra correlations which greatly facilitate interpretation of the dithioacyl enzyme RR spectra. At the same time, we are able to extract dynamical information on the chemical

* To whom correspondence should be addressed.

† Issued as NRCC publication No. 34329.

‡ Institute for Environmental Chemistry, NRC.

(1) Storer, A. C.; Murphy, W. F.; Carey, P. R. *J. Biol. Chem.* **1979**, *254*, 3163–3165.

(2) (a) Carey, P. R.; Storer, A. C. *Acc. Chem. Res.* **1983**, *16*, 455–460.

(b) Carey, P. R.; Storer, A. C. *Annu. Rev. Biophys. Bioeng.* **1984**, *13*, 25–49.

(c) Carey, P. R. In *Biological Applications of Raman Spectroscopy*; Spiro, T. G., Ed.; John Wiley: New York, 1987; Vol. 2, Chapter 6.

(3) Lowe, G.; Williams, A. *Biochem. J.* **1965**, *96*, 189–193.

(4) Kim, M.; Carey, P. R. *J. Mol. Struct.* **1991**, *242*, 421–431.

(5) Huber, C. P.; Ozaki, Y.; Pliura, D. H.; Storer, A. C.; Carey, P. R. *Biochemistry* **1982**, *21*, 3109–3115.

(6) Varughese, K. I.; Storer, A. C.; Carey, P. R. *J. Am. Chem. Soc.* **1984**, *106*, 8252–8257.

reaction by comparing crystal structure results of the model compounds.^{7,8}

In this paper we discuss the crystallographic data for six *N*-acylglycine ethyl dithioesters. They reveal a strong correlation between structural parameters in the -NHCH₂C(=S)SCH₂CH₃ core. These correlations provide novel information on how dynamical excursions occur in this core in *N*-acylglycine dithioacylpapains. The structural data for the ethyl dithioesters also provide the basis for a precise analysis of geometry about the -NHCH₂C(=S)SCH₂ linkages in functioning *N*-benzoylglycine dithioacylpapain. Recently, we derived approximate values of these torsion angles to give the model depicted in Figure 1.⁴ In the present publication we expand considerably the number of marker bands used to obtain structural information, and we provide quantitative values of ϕ' and ψ' for the first time. Interestingly, the value for ψ' is outside the range found in model *N*-benzoylglycine ethyl dithioesters and suggests a modest distortion of ψ' toward the value predicted for the transition state for deacylation.

Experimental Section

The ethyl dithioesters *N*-benzoylglycine ethyl dithioester, *N*-(*p*-methylbenzoyl)glycine ethyl dithioester, and *N*-(*p*-chlorobenzoyl)glycine ethyl dithioester were prepared by the procedure described previously.⁹ The purity of the ethyl dithioesters was checked by NMR, and the results of elemental analysis agreed within acceptable limits (± 0.02 times calculated percentage) with theoretical values.

Yellow crystals of the ethyl dithioesters were obtained by slowly diffusing hexane into solutions of the compounds in ether. Crystals of *N*-(*p*-methylbenzoyl)glycine ethyl dithioester (C₁₂H₁₅NOS₂) belong to the orthorhombic space group *Pbca*. A crystal measuring 0.20 × 0.20 × 0.18 mm³ was mounted on an Enraf-Nonius CAD-4 diffractometer; it provided the following data: $a = 9.7843(14)$, $b = 13.0059(22)$, and $c = 20.913(4)$ Å, $V = 2661.3(8)$ Å³, $\rho = 1.265$ g cm⁻³, $Z = 8$ (21 °C; Cu K α_1 , $\lambda = 1.54056$ Å); $F(000) = 1072.0$, $\mu = 34.1$ cm⁻¹.

Cell dimensions were determined from angular settings of 24 high-order reflections. X-ray intensities were measured in two octants with Ni-filtered Cu K α radiation, using $\omega/2\theta$ scans with variable scan ranges and speeds. There were 1367 unique reflections ($2\theta \leq 100^\circ$), of which 944 with $I \geq 2.5\sigma(I)$ were considered observed. The intensities were corrected for Lorentz and polarization factors; absorption corrections were considered unnecessary. The structure was determined by direct methods with the aid of the computer program MULTAN78.¹⁰ Atomic coordinates and anisotropic temperature parameters of non-hydrogen atoms were refined by full-matrix least-squares analysis. Most hydrogen atoms were located on difference Fourier maps, and the rest were placed in calculated positions; their parameters were not refined. The atomic scattering factors were taken from the *International Tables for X-ray Crystallography*. Throughout the refinement the function $\sum w(|F_o| - |F_c|)^2$ was minimized. The following weighting scheme was used during the final stages: $w = 1$ for $|F_o| \leq 40$, $w = 1/|F_o|^{0.6}$ for $|F_o| > 40$. This scheme made the average values of $w(\Delta F^2)$ independent of $|F_o|$. The conventional residual index R is 0.044, and the weighted index R_w is 0.058 for 933 observed reflections (11 low-order reflections suffered from secondary extinction and were given zero weights). A final difference Fourier map showed no significant features.

(7) Dunitz, J. D. *X-ray Analysis and the Structure of Organic Molecules*; Cornell University: Ithaca, NY, 1979.

(8) Bürgi, H. B.; Dunitz, J. D. *Acc. Chem. Res.* 1983, 16, 153-161.

(9) Storer, A. C.; Ozaki, Y.; Carey, P. R. *Can. J. Chem.* 1982, 60, 199-209.

(10) Main, P.; Hull, S. E.; Lessinger, L.; Germain, G.; DeClercq, J.-P.; Woolfson, M. M. *MULTAN78*, A System of Computer Programs for the Automatic Solution of Crystal Structures from X-ray Diffraction Data; University of York, York, England, and University of Louvain, Louvain, Belgium, 1978.

Lists of final atomic coordinates and anisotropic temperature parameters and of observed and calculated structure factors are available as supplementary material (see paragraph at end of the paper).

Papain, which was purchased from Sigma, was purified on an agarose mercurial column and then by ion-exchange HPLC as described previously.⁴ The enzyme prepared in this way was found to contain $\geq 94\%$ of active cysteine per mole of protein. Acyl enzyme was prepared by mixing, typically, 100 μ L of 50 mM *N*-benzoylglycine methyl thioester substrates (in 50% CH₃CN/H₂O) and 400 μ L of papain (250 μ M, pH 6.5, phosphate buffer) in a rectangular Suprasil cell.

The RR spectra, excited by a 324.0-nm line from a Coherent Radiation Model CR-3000K Kr⁺ laser, were measured using a Spex 1877 Triplemate equipped with a PAR 1421B-1024-HQ intensified photodiode array and a PAR 1460 system processor.^{4,11} For the crushed single crystals in a KBr matrix, the RR scattered light was collected in a 180° backscattering geometry using an Anagrain Anaspec Cassegrain-type collection optic. Reproducible RR spectra of the crushed crystals were obtained using a homemade rotating device.¹² A 0.5-in.-diameter two-layer pellet, which typically consisted of 100 μ g of sample in 30 mg of KBr matrix as the top layer and 270 mg of KBr as the supporting bottom layer, was mounted onto the rotating device. A defocused vertical irradiation area was obtained on the pellet using a cylindrical lens, $f = 120$ mm. For the *N*-benzoylglycine dithioacylpapain intermediate, the RR photons were collected in a 135° backscattering geometry using a focused laser beam. The 135° backscattering geometry served to decrease the background level of the observed RR spectrum and results in a dramatic increase in the signal-to-noise ratio. The spectra were recorded with an entrance slit of 200 μ m for the dispersion stage of Triplemate, giving rise to a spectral width of 6.5 cm⁻¹ for 324.0-nm excitation. For solid samples, wavenumber calibration was made using Raman bands of L-alanine in the solid state and then double-checked using a 337.5-nm laser plasma line equivalent to 1238.5 cm⁻¹ for 324.0-nm excitation. For solution samples, including the enzyme-substrate intermediates, the RR spectra were calibrated using the Raman bands of cyclohexane. The peak positions of the RR bands were reproducible with a precision of ± 1 cm⁻¹.

Results and Discussion

Crystallographic Results for *N*-(*p*-Methylbenzoyl)glycine Ethyl Dithioester. For *N*-(*p*-methylbenzoyl)glycine ethyl dithioester, the bond distances, bond angles, selected torsion angles, mean plane calculations, and hydrogen bond geometries are given in Table I. A stereoscopic diagram with atomic numbering is shown in Figure 2.

The first important feature of the structure is that the molecule takes up a B-type conformation⁵ in the crystalline state. Conformer B is characterized by a small S1C3—C4N1 torsion angle (designated as ψ' and equaling 1.6° for this molecule) and by the orientation of the amide plane nearly orthogonal to the dithioester plane. The B-type conformation has already been found in seven other crystal structures from four different glycine-based dithioesters,^{5,6,13} and two glycine-based thioesters.¹⁴ The most important factor for stabilizing the conformer B has been found to be the nonbonded N1...S1 contact.^{5,6,14} The observed N1...S1 distance in the above dithioesters and thioesters ranges from 2.846 to 2.900 Å^{5,6,13} and from 2.879 to 2.930 Å,¹⁴ respectively. In every case the observed nonbonded distances are shorter than

(11) Carey, P. R.; Sans Cartier, L. R. *J. Raman Spectrosc.* 1983, 14, 271-275.

(12) Kim, M.; Carey, P. R., unpublished work; the drawing is available on request.

(13) Huber, C. P. *Acta Crystallogr.* 1987, C43, 902-904.

(14) Huber, C. P.; Carey, P. R.; Hsi, S.-C.; Lee, H.; Storer, A. C. *J. Am. Chem. Soc.* 1984, 106, 8263-8268.

Table I. Molecular Geometry for *N*-(*p*-Methylbenzoyl)glycine Ethyl Dithioester

Bond Distances (Å)			
S(1)—C(2)	1.802(7)	C(5)—C(6)	1.476(9)
S(1)—C(3)	1.697(6)	C(6)—C(7)	1.401(9)
S(2)—C(3)	1.621(6)	C(6)—C(11)	1.407(9)
O(1)—C(5)	1.232(8)	C(7)—C(8)	1.371(10)
N(1)—C(4)	1.439(8)	C(8)—C(9)	1.391(11)
N(1)—C(5)	1.343(9)	C(9)—C(10)	1.368(14)
C(1)—C(2)	1.491(12)	C(9)—C(12)	1.500(11)
C(3)—C(4)	1.531(9)	C(10)—C(11)	1.374(12)
Bond Angles (deg)			
C(2)—S(1)—C(3)	104.3(3)	C(5)—C(6)—C(7)	123.1(5)
C(4)—N(1)—C(5)	122.0(5)	C(5)—C(6)—C(11)	119.6(6)
S(1)—C(2)—C(1)	114.4(5)	C(7)—C(6)—C(11)	117.2(6)
S(1)—C(3)—S(2)	127.8(4)	C(6)—C(7)—C(8)	121.1(6)
S(1)—C(3)—C(4)	113.8(4)	C(7)—C(8)—C(9)	121.2(7)
S(2)—C(3)—C(4)	118.4(4)	C(8)—C(9)—C(10)	117.8(7)
N(1)—C(4)—C(3)	114.5(5)	C(8)—C(9)—C(12)	120.3(8)
O(1)—C(5)—N(1)	119.8(6)	C(10)—C(9)—C(12)	121.9(8)
O(1)—C(5)—C(6)	122.0(6)	C(9)—C(10)—C(11)	122.4(7)
N(1)—C(5)—C(6)	118.1(5)	C(6)—C(11)—C(10)	120.2(6)
Selected Torsion Angles (deg)			
C(3)—S(1)—C(2)—C(1)	-85.6	C(2)—S(1)—C(3)—S(2)	-1.0
C(2)—S(1)—C(3)—C(4)	179.1	C(5)—N(1)—C(4)—C(3)	-93.6
C(4)—N(1)—C(5)—O(1)	2.8	C(4)—N(1)—C(5)—C(6)	-178.8
S(1)—C(3)—C(4)—N(1)	1.6	S(2)—C(3)—C(4)—N(1)	-178.3
O(1)—C(5)—C(6)—C(7)	-165.1	O(1)—C(5)—C(6)—C(11)	12.2
N(1)—C(5)—C(6)—C(7)	16.5	N(1)—C(5)—C(6)—C(11)	-166.2
Distances (Å) of Atoms to Least-Squares Planes			
Plane I:	S(1) 0.000(3), S(2) 0.000(3), C(3) 0.001(6), C(4) 0.000(9)		
Plane II:	O(1) -0.002(6), N(1) -0.002(7), C(5) 0.009(7), C(6) -0.002(8)		
Plane III:	C(6) -0.006(7), C(7) 0.005(8), C(8) -0.001(9), C(9) 0.002(12), C(10) -0.008(11), C(11) 0.010(9)		
Hydrogen Bond Geometry ^a			
N(1)···O'	2.825(7) Å	H···O' _{corr}	1.81 Å
N(1)—H···O'	159°		

^a The N—H bond was normalized to 1.04 Å.

the sum of sulfur and nitrogen van der Waals radii (3.35 Å¹⁵). For *N*-(*p*-methylbenzoyl)glycine ethyl dithioester discussed here, the N1···S1 distance is 2.825 Å, which is the shortest so far observed for this type of molecule.

The nonbonded contact of amide nitrogen (N1) with thiol sulfur (S1), for both dithioesters and thioesters, has been discussed within the framework of the directional preference of a nucleophile approaching divalent sulfur^{5,16} that was originally proposed by Rosenfield, Parthasarathy, and Dunitz¹⁶ for other systems. The nucleophilic amide nitrogen approaches the thiol sulfur approximately along the extension of the S1—C2 bond (N1···S1—C2). Two qualitative interpretations of this interaction have been given in terms of MO theory.⁶ One is that a HOMO localized on the amide nitrogen (N1) overlaps with a LUMO σ^* based on the S1—C2 fragment. The other is that the lone-pair electrons on the amide nitrogen interact with the sulfur d orbitals. As has been pointed out in previous publications from this laboratory, both effects should be taken into account.

Another interesting structural feature observed in *N*-(*p*-methylbenzoyl)glycine ethyl dithioester is that the molecule takes up a near-*gauche* conformation ($\chi_2 = -85.6^\circ$) about the C1C2—S1C3 single bond. Such a large deviation in the torsion angle from *gauche* ($\pm 60^\circ$) can be explained in terms of the repulsion between the thiono sulfur, S2, and a methylene hydrogen of -C₂H₅. In fact, the nonbonded S2···H distance is 2.662 Å, which is much shorter than the sum of S and H van der Waals radii (3.00 Å¹⁵).

In Table II, selected structural parameters from six different molecules of *N*-acylglycine ethyl dithioesters are listed in order

of increasingly positive ψ /(S1C3—C4N1) torsion angles. For the first four compounds, where the ψ angle is negative, *trans* conformations about the C1C2—S1C3 bond (χ_2) are seen, whereas for the last two compounds, where the ψ angle is positive, *gauche* conformations about this bond are seen. Although in the crystal state torsion angles can be easily altered by crystal packing forces,¹⁷ it is tempting to suggest that the C3S1—C2C3 single bond switches from *trans* to *gauche* conformation when the ψ torsion angle changes from negative to positive. In all likelihood, this conformational preference is associated with the directional preference of the N1···S1 nonbonded interaction.

Structural Correlations for *N*-Acylglycine Ethyl Dithioesters.

In order to elucidate correlated structural changes in the common skeleton of *N*-acylglycine ethyl dithioesters, C5(=O)N1C4C3-(=S2)S1C2C1, an extensive comparison was made among the above-mentioned six molecules of B-type *N*-acylglycine ethyl dithioesters with respect to bond lengths, bond angles, torsion angles, and nonbonded distances (Table II). The most significant insight emerging from the comparison is that the central N1—C4—C3—S1 skeleton changes geometry as the ψ -(S1C3—C4N1) torsion angle is altered from -22.2 to +9.5°. As is shown in Figure 3, the length of the central C3—C4 bond is elongated and then contracted, with increasingly positive values of the ψ torsion angle. Concomitantly, the β (C3—C4—N1) bond angle decreases and then increases, whereas the α (S1—C3—C4) bond angle remains essentially unchanged. Simple geometric considerations can predict the nonbonded N1···S1 distances as a function of the ψ torsion angle. For *N*-acetylglycine ethyl dithioester and *N*-(β -phenylpropionyl)glycine ethyl dithioester, the N1···S1 nonbonded distances are calculated to be 2.839 and 2.863 Å, respectively, when ψ is rotated to 0° and other structural parameters are kept constant. Both distances are longer than 2.825 Å in *N*-(*p*-methylbenzoyl)glycine ethyl dithioester. The further shortening of the N1···S1 distance for the latter dithioester is mainly due to the change in the β angle. Figure 4 (top) shows that the β bond angle decreases as N1 comes closer to S1 in *N*-acylglycine ethyl dithioesters. Obviously, this provides additional compelling evidence that the N1···S1 nonbonded interaction is attractive in nature.

Another interesting correlation involving the N1···S1 nonbonded distance is, as shown in Figure 4 (bottom), that the C3—C4 bond length is elongated from 1.504 to 1.531 Å as the nonbonded distance shortens from 2.900 to 2.825 Å. The most likely explanation of this observation is that the N1···S1 nonbonded attractive interaction reduces the β angle, resulting in increasing repulsion between N1 and C3 atoms (1,3-interaction). This repulsion then gives rise to lengthening of the C3—C4 linkage. Accordingly, the geometry of the N1—C4—C3—S1 skeleton is determined mainly by a balance between the N1···S1 attractive and the N1···C3 repulsive intramolecular interactions. Another, less likely, interpretation is that the lengthening is due to a through-bond interaction.¹⁸ For example, in *p,p'*-dibenzene,¹⁹ the through-bond interaction proves to be responsible for a significant elongation of the C—C σ bond, intervening between the properly aligned π ring systems. For the molecules discussed here, however, it seems unlikely that the C3—C4 bond is lengthened by the interaction between delocalized π -electrons on the amide plane and those on the dithioester plane, which are oriented nearly orthogonally to each other.

A well-established correlation found in earlier studies^{6,14} on *N*-acylglycine ethyl dithioesters is the linear relationship between the ψ /(S1C3—C4N1) and ϕ' (C3C4—N1C5) torsion angles, which is shown in Figure 5. Originally, it was shown that the

(17) For example: Pierrot, M.; Estienne, J. In *Structure and Properties of Molecular Crystals*; Pierrot, M., Ed.; Elsevier: New York, 1990; Chapter 1.

(18) For reviews: (a) Hoffmann, R. *Acc. Chem. Res.* 1971, 4, 1–9. (b) Gleiter, R. *Angew. Chem., Int. Ed. Engl.* 1974, 13, 696–701.

(19) Dougherty, D. A.; Schlegel, H. B.; Mislow, K. *Tetrahedron* 1978, 34, 1441–1447.

(15) Bondi, A. *J. Phys. Chem.* 1964, 68, 441–451.

(16) Rosenfield, R. E., Jr.; Parthasarathy, R.; Dunitz, J. D. *J. Am. Chem. Soc.* 1977, 99, 4860–4862.

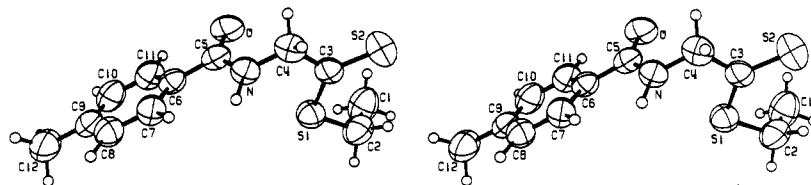


Figure 2. Stereoscopic diagram of *N*-(*p*-methylbenzoyl)glycine ethyl dithioester with the labeling scheme. Thermal ellipsoids are drawn at the 50% probability level.

Table II. Selected Bond Lengths (Å), Bond Angles (deg), and Torsion Angles (deg) of Crystalline *N*-Acylglycine Ethyl Dithioesters

compd	C2—S1	S1—C3	C3=S2	C3—C4	C4—N1	α^a	β^b	ψ^c	ϕ^d	χ_2^e	N1...S1 ^f
AG ^a	1.807(9)	1.700(6)	1.635(5)	1.504(11)	1.444(6)	114.2(4)	115.7(5)	-22.2	-76.3	-168.5	2.891
PPG ^b	1.807(3)	1.704(2)	1.624(3)	1.507(4)	1.443(3)	114.2(2)	116.6(2)	-18.9	-75.4	+179.2	2.900
BGX ^c	1.804(3)	1.710(3)	1.615(3)	1.522(3)	1.446(3)	113.8(3)	115.2(3)	-15.5	-78.7	-176.1	2.866
BGY ^d	1.804(3)	1.711(3)	1.624(3)	1.522(3)	1.453(3)	114.1(3)	114.5(3)	-10.5	-83.5	+178.8	2.846
MBG ^e	1.802(7)	1.697(6)	1.621(6)	1.531(9)	1.439(8)	113.8(4)	114.5(5)	+1.6	-93.6	-85.6	2.825
CBG ^f	1.820(3)	1.710(3)	1.618(3)	1.518(3)	1.447(3)	113.5(3)	115.8(3)	+9.5	-97.1	-88.7	2.851

^a AG, *N*-acetylglycine ethyl dithioester; from ref 5. ^b PPG, *N*-(β -phenylpropionyl)glycine ethyl dithioester; from ref 13. ^c BGX, *N*-benzoyl glycine ethyl dithioester, Mol-X; from ref 6. ^d BGY, *N*-benzoyl glycine ethyl dithioester, Mol-Y; from ref 6. ^e MBG, *N*-(*p*-methylbenzoyl)glycine ethyl dithioester; from this work. ^f CBG, *N*-(*p*-chlorobenzoyl)glycine ethyl dithioester; from ref 6. ^g Bond angle (S1—C3—C4). ^h Bond angle (C3—C4—N1). ⁱ Torsion angle (S1C3—C4N1). ^j Torsion angle (C3C4—N1C5). ^k Torsion angle (C1C2—S1C3). ^l N1...S1 nonbonded distance.

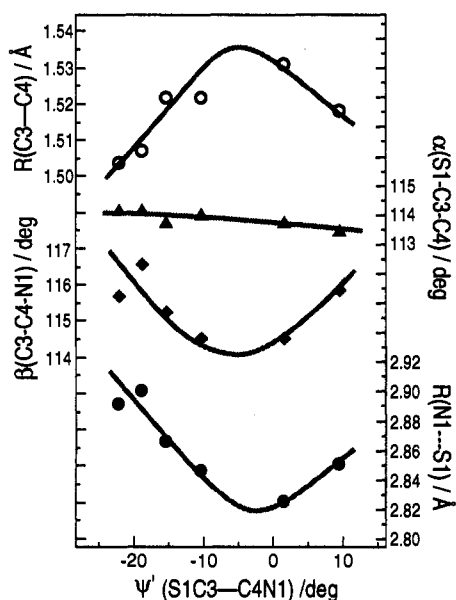


Figure 3. Plots of the C3—C4 bond length, the α (S1—C3—C4) bond angle, the β (C3—C4—N1) bond angle, and the N1...S1 nonbonded distance versus the ψ' (S1C3—C4N1) torsion angle.

(ψ' , ϕ) values lie on a straight line for four different *N*-acylglycine ethyl dithioesters (AG, BGX, BGY, and CBG; see the caption to Table II for these abbreviations).⁶ This was successfully explained in terms of what is called the "θ valley".⁶ The angle θ , defined as the angle between the N1...S1 direction and the normal to the amide plane, is kept nearly constant (between 20.1 and 22.1°) in the ψ' angle region from -22.2 to +9.5°. The (ψ' , ϕ) angles of *N*-(*p*-methylbenzoyl)glycine ethyl dithioester (MBG) determined here, as well as those of *N*-(β -phenylpropionyl)glycine ethyl dithioester (PPG),¹³ are now included in Figure 5. The straight line was determined by the least-squares method using all six crystal data sets.

A comparison of the structural parameters of *N*-(*p*-methylbenzoyl)glycine ethyl dithioester with those of the other five *N*-acylglycine ethyl dithioesters^{5,6,13} allows us to take the following view regarding the structural changes about the central skeleton. The amide nitrogen appears to revolve around the sulfur of the ester link through an elliptical-like orbit, in the small ψ' region, with the amide N p orbital favoring approach to the thiol S1 along the θ valley. As the amide nitrogen approaches the thiol sulfur due to the attractive N1...S1 nonbonded interaction, the

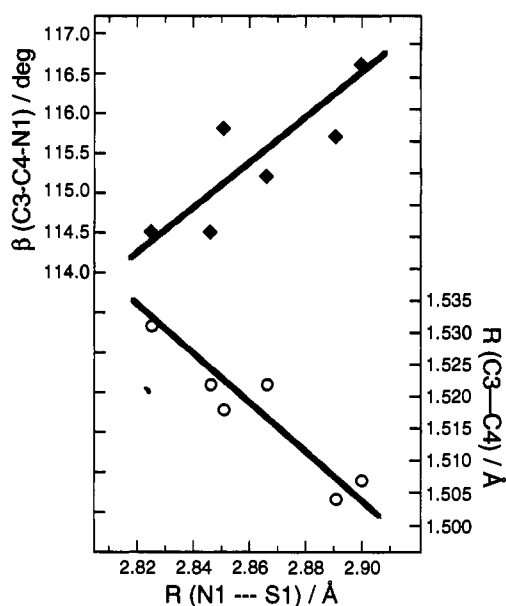


Figure 4. Plots of the C3—C4 bond length and the β (C3—C4—N1) bond angle versus N1...S1 nonbonded distance.

β angle is appreciably narrowed, and therefore the C3—C4 bond is substantially elongated. Additionally, the conformational preference about the C3S1—C2C1 single bond, *trans* or *gauche*, is probably associated with the position of the amide nitrogen.

The above considerations provide important insight into the reaction pathway of acylpapain intermediates. The latter lie between the acylation and deacylation reaction steps of the enzyme. As the acyl enzyme undergoes thermal fluctuations about its equilibrium geometry in preparation for excursions along the reaction pathway, it is likely that correlated changes in the acyl enzyme bonds, viz. the N...S nonbonded distance, the β angle, and the C3—C4 bond length, occur in the active site as detailed here for the model compounds. Thus, each N1—C4—C3—S1 framework structure detailed above can be regarded as a "snapshot" of dithioacylpapain intermediates in conformational space near the dithioacylpapain energy minimum.⁸ The series of six structures provides a six-frame motion picture of reaction dynamics involving correlated structural changes about the dithioacylpapain minimum.

Structure-Spectra Correlations for *N*-Acylglycine Ethyl Dithioesters. The 324-nm excited resonance Raman spectrum from crystals of *N*-(*p*-methylbenzoyl)glycine ethyl dithioester in

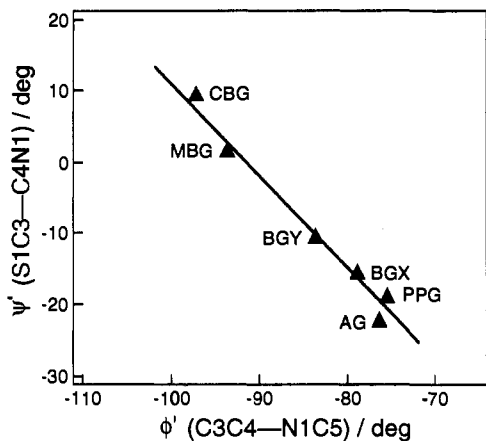


Figure 5. Correlation between $\psi'(S1C3-C4N1)$ and $\phi'(C3C4-N1C5)$ torsion angles.

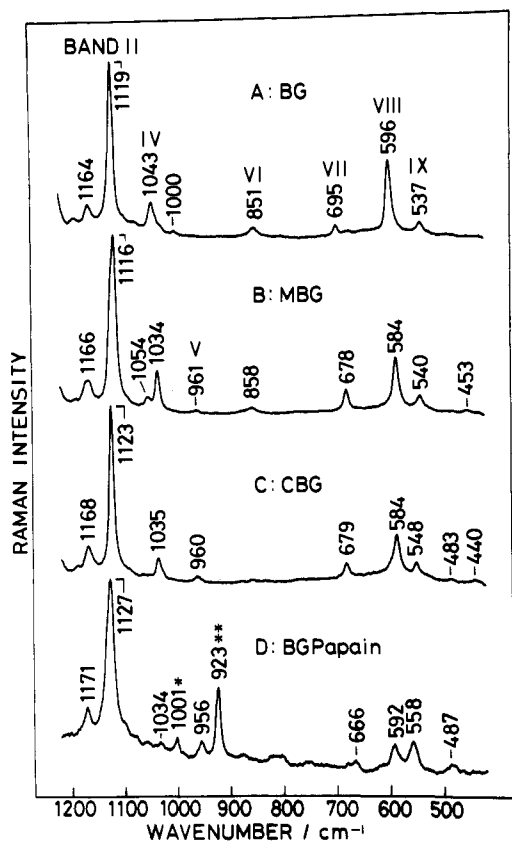


Figure 6. Comparison of the RR spectra of *N*-benzoylglycine ethyl dithioesters in crystalline states and dithioacylpapain in 10% CH_3CN/H_2O solution in the 420–1220- cm^{-1} region: (A) *N*-benzoylglycine ethyl dithioester; (B) *N*-(*p*-methylbenzoyl)glycine ethyl dithioester; (C) *N*-(*p*-chlorobenzoyl)glycine ethyl dithioester; (D) *N*-benzoylglycine dithioacylpapain. Spectral conditions for *N*-benzoylglycine ethyl dithioesters in the crystalline state: 324-nm excitation (20 mW), 180° backscattering from spinning KBr pellet, $6.5\text{-}cm^{-1}$ experimental resolution, 72-s data acquisition time (18 scans of 4-s exposure). Spectral conditions for *N*-benzoylglycine dithioacylpapain in 10% CH_3CN/H_2O solution: 324-nm excitation (15 mW), 135° backscattering, $6.5\text{-}cm^{-1}$ experimental resolution, 120-s data acquisition time (30 scans of 4-s exposure).

the 400–1300- cm^{-1} region is seen in Figure 6. Successive improvements of a microsampling method for solid-state samples allow us to record a high-quality resonance Raman spectrum from as little as 100 μg of small crystals in a KBr matrix. Thus, resonance Raman spectroscopy could be carried out on crushed single crystals from the same batch as that used to provide samples for X-ray crystallographic analysis. There is good evidence, based on the "normal" red-excited Raman spectra of single crystals and

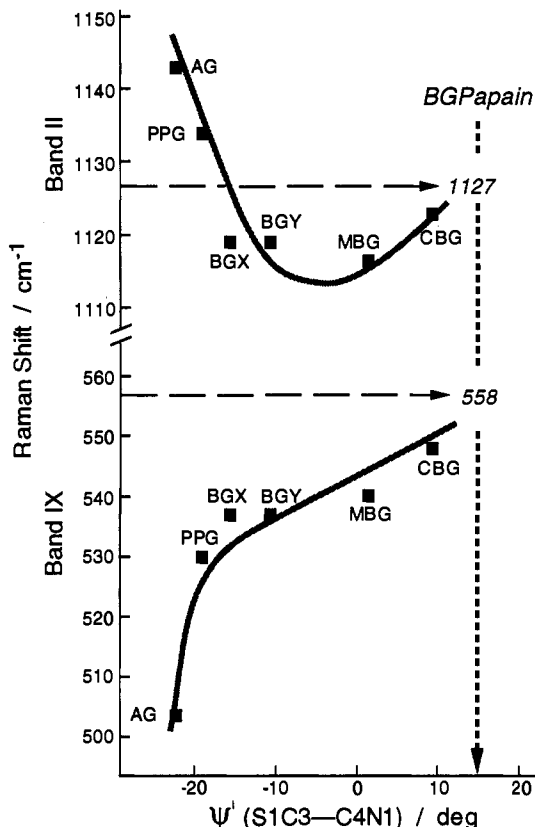


Figure 7. Variations of Band II and Band IX relative to the torsion angle $\psi'(S1C3-C4N1)$ for six different single crystals of *N*-acylglycine ethyl dithioesters: AG, *N*-acetyl glycine ethyl dithioester; PPG, *N*-(β -phenylpropionyl)glycine ethyl dithioester; BGX, *N*-benzoylglycine ethyl dithioester, Mol-X; BGY, *N*-benzoylglycine ethyl dithioester, Mol-Y; MBG, *N*-(*p*-methylbenzoyl)glycine ethyl dithioester; CBG, *N*-(*p*-chlorobenzoyl)glycine ethyl dithioester.

powders, that the conformation of dithioesters in the crystal is retained upon grinding to a powder.^{20,21}

As Figure 6B shows, the resonance Raman spectrum of *N*-(*p*-methylbenzoyl)glycine ethyl dithioester gives rise to a prominent band at 1116 cm^{-1} , designated as Band II.² The wavenumber value is the lowest among the *N*-acylglycine ethyl dithioesters so far examined. Much effort has been made toward characterizing the vibrational mode of Band II, using infrared, normal Raman, and resonance Raman spectroscopies for a series of *N*-acylglycine ethyl dithioesters and their isotopically substituted analogues^{22,23} and employing normal coordinate calculations on simple dithioacetates.^{24,25} Essential findings derived from the earlier studies on Band II are as follows. First, Band II is ascribable mainly to C3=S2 and C3-C4 stretching vibrations of the -C4-C3(=S2)-fragment. Second, the peak position of Band II is sensitive to changes in the two torsion angles about the glycinic linkages (ψ' , ϕ') but shows less sensitivity to torsion angle variation about the C2-S1 bond (χ_2).

Figure 7 (top) demonstrates a correlation between the resonance Raman peak position of Band II and the $\psi'(S1C3-C4N1)$ torsion angle for six crystallographically distinct *N*-acylglycine ethyl

(20) Varughese, K. I.; Angus, R. H.; Carey, P. R.; Lee, H.; Storer, A. C. *Can. J. Chem.* **1986**, *64*, 1668–1673.

(21) Angus, R. H.; Carey, P. R.; Lee, H.; Storer, A. C.; Varughese, K. I. *Can. J. Chem.* **1985**, *63*, 2169–2175.

(22) Storer, A. C.; Ozaki, Y.; Carey, P. R. *Can. J. Chem.* **1982**, *60*, 199–209.

(23) Lee, H.; Storer, A. C.; Carey, P. R. *Biochemistry* **1983**, *22*, 4781–4789.

(24) Teixeira-Dias, J. J. C.; Jardim-Barreto, V. M.; Ozaki, Y.; Storer, A. C.; Carey, P. R. *Can. J. Chem.* **1982**, *60*, 174–189.

(25) Jardim-Barreto, V. M.; Teixeira-Dias, J. J. C.; Carey, P. R.; Storer, A. C. *Port. J. Chem.* **1984**, *26*, 131–142.

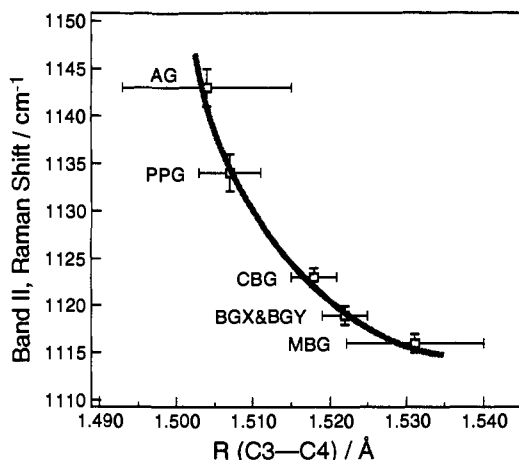


Figure 8. Plots of the Band II wavenumber versus the C3—C4 bond length.

dithioesters. Careful measurements, with a wavenumber precision of ± 0.5 cm^{-1} for Band II, have now been performed for crystals of substituted and unsubstituted *N*-benzoylglycine ethyl dithioesters (BGX and BGY, MBG and CBG; for these abbreviations, see the caption to Table II). Two other data for *N*-acylglycine ethyl dithioesters (AG and PPG; see the caption to Table II) were taken from unpublished Raman spectra obtained in this laboratory. As is evident from Figure 7 (top), Band II is downshifted and then upshifted as the ψ' torsion angle about the C3—C4 single bond becomes increasingly positive in the region between -22.2 and $+9.5^\circ$.

Among many factors that might influence the peak position of a vibrational mode, changes in the structural parameters associated with the mode bring about changes in the potential energy of the molecule, resulting in shifting of the observed peak position.²⁶ In Figure 8, the observed positions of Band II are plotted against the bond lengths of the C3—C4 single bond determined by X-ray crystallography for each *N*-acylglycine ethyl dithioester (Table II). The peak position appears to be well correlated with the bond length of the C3—C4 single bond. Specifically, as the C3—C4 bond lengthens from 1.504 to 1.531 Å, the peak position of Band II downshifts from 1143 to 1116 cm^{-1} . Thus, the downshift of Band II can be mainly ascribed to the elongation of the C3—C4 single bond, i.e., to bond weakening. This provides a good explanation as to why Band II for *N*-(*p*-methylbenzoyl)glycine ethyl dithioester is observed at the lowest wavenumber, 1116 cm^{-1} : this compound has the longest C3—C4 bond length. As illustrated above, the C3—C4 bond length correlates with the ψ' (S1C3—C4N1) torsion angle (Figure 3, top). This provides a rationale for why the peak position of Band II correlates with the ψ' (S1C3—C4N1) torsion angle in the manner shown in Figure 7 (top), where the wavenumber decreases with increasing torsion angle, reaches a minimum near 0° , and then increases. As demonstrated above, there are clear correlations involving the C3—C4 bond length, the β (C3—C4—C1) bond angle, and ψ' (S1C3—C4N1) and ϕ' (C3C4—N1C5) torsion angles. This leads us to the more general conclusion that the wavenumber of Band II is a sensitive monitor of the structural changes seen around the -C5(=O)N1C4C3(=S2)S1 fragment of *N*-acylglycine ethyl dithioesters.

Conformation about the Acyl—Glycine Linkages of the Papain Intermediate. Parts A, B and C of Figure 6 show 324-nm-excited RR spectra from crushed single crystals of *N*-benzoylglycine ethyl dithioester, *N*-(*p*-methylbenzoyl)glycine ethyl dithioester, and *N*-(*p*-chlorobenzoyl)glycine ethyl dithioester, respectively. These RR spectra bear some similarity, but each spectrum is distinctive in terms of exact peak positions and relative intensities throughout

the whole spectral region. Part D of Figure 6 shows the 324-nm-excited RR spectrum of *N*-benzoylglycine papain in a 10% $\text{CH}_3\text{CN}/\text{H}_2\text{O}$ solution. As is evident, all RR bands arising from the enzyme—substrate intermediates, observed at 1171, 1127, 1034, 956, 666, 592, 558, and 487 cm^{-1} , have their counterparts in the spectra of the model compounds. The RR bands near 1040, 960, 850, 690, 590, and 550 cm^{-1} are designated as Bands IV, V, VI, VII, VIII, and IX, respectively (Bands I, II, and III were designated as the features near 1170, 1130, and 1080 cm^{-1} , respectively, in earlier studies from this laboratory²⁷).

As discussed above, the peak position of Band II, which is observed at 1119, 1116, and 1123 cm^{-1} in Parts A, B, and C in Figure 6, respectively, is sensitive to the correlated structural changes seen within the C5(=O)N1C4C3(=S2)S1C2C1 fragment²⁸ of *N*-acylglycine ethyl dithioesters. Specifically, the frequency of Band II downshifts and then upshifts as the ψ' -(S1C3—C4N1) torsion angle becomes increasingly positive. For the dithioacylpapain intermediate (Figure 6D), Band II is seen at 1127 cm^{-1} . If the correlation between Band II and the ψ' -(S1C3—C4N1) torsion angle is directly transferred to the dithioacylpapain intermediate, ψ' for the intermediate cannot be determined unequivocally. As is demonstrated in Figure 7 (top), there are two possible values of the ψ' torsion angle, approximately $+15^\circ$ or -15° , prompting us to search for correlations between ψ' and other RR bands.

The RR spectrum of *N*-benzoylglycine ethyl dithioester (Figure 6A) gives rise to Band IX at 537 cm^{-1} . The band upshifts to 540 cm^{-1} in the spectrum of *N*-(*p*-methylbenzoyl)glycine ethyl dithioester (Figure 6B) and then to 548 cm^{-1} in the spectrum of *N*-(*p*-chlorobenzoyl)glycine ethyl dithioester (Figure 6C). These data, together with positions of Band IX for *N*-acetylglycine ethyl dithioester (AG) and *N*-(β -phenylpropionyl)glycine ethyl dithioester (PPG),²⁹ are plotted against the ψ' (S1C3—C4N1) torsion angle in Figure 7 (bottom). The data strongly suggest that as ψ' becomes increasingly positive, Band IX shifts to higher frequency. It should be noted that Band IX is not seen in the RR spectrum of methyl dithioacetate ($\text{CH}_3\text{C}(=\text{S})\text{SCH}_3$) or ethyl dithioacetate ($\text{CH}_3\text{C}(=\text{S})\text{SCH}_2\text{CH}_3$),²⁴ whereas the band is observed for the above five *N*-acylglycine ethyl dithioesters. Therefore, Band IX is tentatively assigned to a skeletal deformation, known to be sensitive to conformation,³⁰ of the C5(=O)-N1C4C3(=S2)S1C2C1 fragment.²⁸ Interestingly, Band IX upshifts further to 558 cm^{-1} for the dithioacylpapain intermediate (Figure 6D). By extrapolation of the correlation between Band IX and ψ' in Figure 7 (bottom), the position of Band IX indicates that the ψ' torsion angle for *N*-benzoylglycine dithioacylpapain intermediates is approximately $+15^\circ$ in the enzyme's active site, in good agreement with the value of $|15|^\circ$ determined from Band II. The value of $+15^\circ$ for ψ' of *N*-benzoylglycine dithioacylpapain is appreciably larger than the values for *N*-acylglycine ethyl dithioesters, which fall in the region from -22.2 to $+9.5^\circ$. This conclusion will be supported below by discussion of the relative intensity changes seen in Bands IV, V, and VI.

The RR spectrum of *N*-(*p*-methylbenzoyl)glycine ethyl dithioester (Figure 6B) gives rise to Bands V and VI at 961 and 858 cm^{-1} , respectively. On the basis of the studies of Koyama and Shimanouchi³¹ and Dwivedi and Krimm,³² these bands are ascribed to the CH_2 rocking motions of the C4 methylene bridge

(27) Ozaki, Y.; Pllura, D. H.; Carey, P. R.; Storer, A. C. *Biochemistry* 1982, 21, 3102–3108.

(28) For consistency, the atomic numbering of the *N*-(*p*-methylbenzoyl)glycine ethyl dithioester (Figure 2) was used for *N*-benzoylglycine dithioacylpapain.

(29) Unpublished data from this laboratory.

(30) Mizushima, S.; Shimanouchi, T.; Nakagawa, I.; Miyake, A. *J. Chem. Phys.* 1953, 21, 215–219.

(31) Koyama, Y.; Shimanouchi, T. In *Peptides, Polypeptides and Proteins, Proceedings of the Rehovot Symposium on Poly(Amino Acids), Polypeptides, and Proteins and Their Biological Implications*, 2nd ed.; Blout, E. R., Bovey, F. A., Goodman, M., Eds.; John Wiley: New York, 1974; pp 396–418.

(32) Dwivedi, A. M.; Krimm, S. *Biopolymers* 1982, 21, 2377–2397.

(26) For example: Califano, S. *Vibrational States*; John Wiley: New York, 1976.

that are strongly mixed with skeletal stretching involving, e.g., C3—C4 and N1—C4 stretches. Band V is not seen in the spectrum of *N*-benzoylglycine ethyl dithioester (Figure 6A), but the band is observed distinctly at 960 cm⁻¹ in the spectrum of *N*-(*p*-chlorobenzoyl)glycine ethyl dithioester (Figure 6C). In contrast, Band VI is clearly observed at 851 cm⁻¹ for *N*-benzoylglycine ethyl dithioester, but the band is at best very weak for *N*-(*p*-chlorobenzoyl)glycine ethyl dithioester. It appears from these results that as the ψ (S1C3—C4N1) torsion angle is increased from negative to positive, Band V is enhanced in intensity, while Band VI is diminished in intensity. Interestingly, for *N*-benzoylglycine dithioacylpapain, Band V is observed at 956 cm⁻¹, whereas Band VI is not seen in its frequency region (all minor peaks in the 800–900-cm⁻¹ region in Figure 6D arise from the enzyme itself³³). This spectral change can be explained by assuming that the ψ torsion angle for the enzyme–substrate intermediates is larger than the value of +9.5° for *N*-(*p*-chlorobenzoyl)glycine ethyl dithioester—consistent with the conclusion that the ψ torsion angle is approximately +15° for the enzyme–substrate intermediates, which was deduced from the peak positions of Bands II and IX.

Band IV is observed at 1043 cm⁻¹ in the RR spectrum of *N*-benzoylglycine ethyl dithioester (Figure 6A) and is seen at 1034 and 1035 cm⁻¹ for *N*-(*p*-methylbenzoyl)glycine ethyl dithioester (Figure 6B) and *N*-(*p*-chlorobenzoyl)glycine ethyl dithioester (Figure 6C), respectively. The *N*-benzoylglycine ethyl dithioester molecule takes up a *trans* conformation about the C3S1—C2C1 single bond, while the latter two molecules adopt a *gauche* conformation about the single bond. This suggests that Band IV is sensitive to conformation about the C3S1—C2C1 single bond, *trans* or *gauche*. Since Band IV is seen at 1052 cm⁻¹ for *N*-benzoylglycine methyl dithioester in the solid state (unpublished work, this laboratory), skeletal stretching vibrations, such as N1—C4 and C3—C4 stretching vibrations, probably make appreciable contributions to Band IV. For the dithioacylpapain intermediates, Band IV is observed at 1034 cm⁻¹ as a weak band (Figure 6D). This is additional evidence for a *gauche* conformation about C3S1—C2C1 and supports the conclusion drawn earlier on the basis of analysis of Band VII near 680 cm⁻¹.⁶ Interestingly, when the ψ (S1C3—C4N1) torsion angle is altered from +1.6° (for *N*-(*p*-methylbenzoyl)glycine ethyl dithioester) to +9.5° (for *N*-(*p*-chlorobenzoyl)glycine ethyl dithioester), Band IV reduces in intensity while keeping its frequency near 1034 cm⁻¹ (Figure 6B and C). Thus, the weak band seen in Figure 6D is quite consistent with the above conclusion that the ψ torsion angle is approximately +15° for *N*-benzoylglycine dithioacylpapain.

As discussed earlier,⁶ a linear relationship exists between the ψ (S1C3—C4N1) and ϕ (C3C4—N1C5) torsion angles for six different *N*-acylglycine ethyl dithioesters in the crystalline state within the ψ torsion angle region from -22.2 to +9.5°. A simple extrapolation of the linearity shows that the ψ torsion angle of +15°, which was estimated for *N*-benzoylglycine dithioacylpapain intermediates above, corresponds to the ϕ ' torsion angle of -105°. Thus, we quantitate the conformation about the glycinic linkages, S1C3—C4N1 and C3C4—N1C5, as (ψ, ϕ) = (+15°, -105°) for the enzyme–substrate intermediate.

Conformation about the Cysteine Linkages. An earlier study²⁴ has shown that an ethyl dithioester vibrational mode, which gives rise to a weak RR band in the 700–675-cm⁻¹ region (Band VII), includes a high degree of S1—C2 stretching character and is sensitive to conformation, *trans* or *gauche*, about the C3S1—C2C1 single bond. For example, as is evident from Figure 6A–C, *trans* (*N*-benzoylglycine ethyl dithioester) and *gauche* conformers (*N*-(*p*-methylbenzoyl)glycine ethyl dithioester and *N*-(*p*-chlorobenzoyl)glycine ethyl dithioester) about the C3S1—C2C1 single bond give rise to Band VII near 695 and near 678 and 679 cm⁻¹,

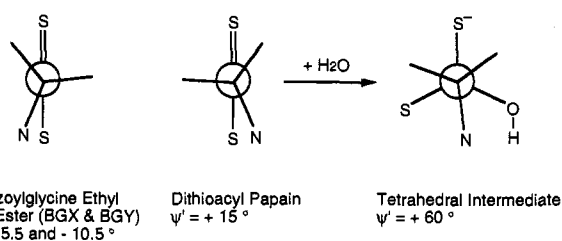


Figure 9. Newman projections along C3—C4 for *N*-benzoylglycine ethyl dithioester, *N*-benzoylglycine dithioacylpapain, and the tetrahedral intermediate for deacylation.

respectively. Thus, Band VII is shown to be a potential marker band for conformation about the C3S1—C2C1 single bond. Recently, we took both cysteine linkages of dithioacylpapain intermediates, χ_1 and χ_2 , into consideration and proposed that the preferred conformation about the cysteine-25 linkages is *gauche*-P_H, where the hydrogen linked to C₂₅^α is in the *trans* position with respect to the thiol sulfur atom (Figure 1).⁴ The conformational analysis was based on the peak position of Band VII near 666 cm⁻¹ observed for *N*-(methoxy)carbonylglycine-phenylalanyl-glycine dithioacylpapain and *N*-(methoxy)carbonylphenylalanyl-glycine dithioacylpapain intermediates. Band VII is also seen at 666 cm⁻¹ for *N*-benzoylglycine dithioacylpapain intermediates in solution (Figure 6D). Thus, we conclude that *N*-benzoylglycine dithioacylpapain also takes up the *gauche*-P_H conformation about the cysteine linkages. As discussed above, the position of Band IV at 1034 cm⁻¹ provides additional support for the *gauche* form.

Fine-Tuned Conformation. An important outcome of the present work is that the ψ (S1C3—C4N1) torsion angle for *N*-benzoylglycine dithioacylpapain is estimated to be approximately +15°. It should be remembered that this value of ψ is very different from those of the corresponding model compounds, *N*-benzoylglycine ethyl dithioesters, -15.5 and -10.5° (BGX and BGY, two crystallographically independent molecules) and is outside the ψ torsion angle region, from -22.2 to +9.5°, so far observed for *N*-acylglycine ethyl dithioesters. In all likelihood, enzyme–substrate contacts, e.g., hydrogen-bonding and hydrophobic interactions, bring about the increase in ψ to approximately +15° in the active site of the enzyme (Figure 9). In particular, hydrogen-bonding interactions involving the amide group of the substrate should play an important role in determining the ψ torsion angle. In the acylpapain structure deduced from X-ray analyses of chloromethyl ketone-inhibited papains, the amide carbonyl group, which corresponds to the C5=O1 group of the compounds discussed here, forms a hydrogen bond with the Gly-66 main-chain NH group, while the amide NH group of the substrate, which corresponds to N1H, does not have a direct hydrogen-bonding partner in the enzyme but is hydrogen-bonded to a water molecule.³⁴ Since the direction of these hydrogen-bonding interactions is nearly orthogonal to the rotation axis of the C3—C4 single bond, we suggest that the value of the ψ (S1C3—C4N1) torsion angle for the acylpapain intermediates is regulated, at least in part, through hydrogen-bonding interactions, which includes the C5=O1 group and/or the N1H group of the substrate. These interactions increase the positive value of ψ , as shown, in going from the left to the middle Newman projection in Figure 9.

A cogent question concerns the possible mechanistic significance of the increase in the ψ (S1C3—C4N1) torsion angle to approximately +15° in the enzyme's active site. A pertinent factor concerns the conformation of the transient tetrahedral intermediate for deacylation,^{35,36} which is close to the deacylation transition state on the reaction pathway. As is shown schemat-

(34) Drenth, J.; Kalk, K. H.; Swen, H. M. *Biochemistry* 1976, 15, 3731–3738.

(35) Szawelski, R. J.; Wharton, C. W. *Biochem. J.* 1981, 199, 681–692.

(36) Storer, A. C.; Carey, P. R. *Biochemistry* 1985, 24, 6808–6818.

(33) Kim, M.; Carey, P. R. unpublished data.

ically in Figure 9 (right), the sterically favored conformation in the tetrahedral intermediate is one in which the S1 atom (thiol sulfur) is in the *gauche*⁺ (ca. +60°) position with respect to the amide N1.³⁶ Thus the observed value of +15° for ψ' in the acyl enzyme represents a small but significant departure of ψ' found in model esters in the direction of ψ' for the transition state and must be driven in this direction by enzyme-substrate contacts. In addition, this fine-tuned conformation serves to decrease the N1...S1 intramolecular attractive interaction in the enzyme's active site and reduce its stabilizing effect on the acyl enzyme energy.

Acknowledgment. We are grateful to Dr. Marianne Pusztai-Carey for preparing *N*-benzoylglycine ethyl dithioester and to Robert Carriere for his assistance in purifying the enzyme. All

crystallographic calculations were performed with the NRCVAX system of programs.³⁷ Figure 2 was drawn with the ORTEP program of Johnson.³⁸ We would like to thank Dr. Xiao-Yuan Li for helpful discussions.

Supplementary Material Available: Final atomic coordinates and anisotropic temperature parameters (2 pages); observed and calculated structure factors for *N*-(*p*-methylbenzoyl)glycine ethyl dithioester (8 pages). Ordering information is given on any current masthead page.

(37) Gabe, E. J.; LePage, Y.; Charland, J. P.; Lee, R. L.; White, P. S. NRCVAX—An Interactive Program System for Structure Analysis. *J. Appl. Cryst.* **1989**, *22*, 384–387.

(38) Johnson, C. K. ORTEP-II. Report ORNL-5138; Oak Ridge National Laboratory: Oak Ridge, TN, 1976.